

Technology developments in laser, detector, and receiver system for an atmospheric CO₂ lidar profiling system

Syed Ismail¹, Grady Koch¹, Nurul Abedin¹, Tamer Refaat², Manuel Rubio¹, Kenneth Davis³, Charles Miller⁴, and Upendra Singh¹

¹NASA Langley Research Center, Hampton, VA

²Old Dominion University, Norfolk, VA

³Pennsylvania State University, University Park, PA

⁴Jet Propulsion Laboratory, California Institute of Technology, Pasadena, CA

Abstract- Technology developments are in progress towards the development of a Differential Absorption Lidar (DIAL) to measure range-resolved and column amounts of atmospheric CO₂. This system is also capable of providing high-resolution aerosol profiles and cloud distributions. It is being developed as part of the NASA ESTO Instrument Incubator Program (IIP). The long-term goal of this work is the development of a space-based DIAL system. The IIP effort involves the design, development, evaluation, and fielding of a ground-based CO₂ profiling system. A successful outcome of this development will be an instrument capable of making measurements in the lower troposphere and boundary layer where the sources and sinks of CO₂ are located. It will also be a valuable tool for contributing to the validation of space-based measurements of column CO₂ from NASA's Orbiting Carbon Observatory (OCO) and for participation in the North American Carbon Program (NACP) regional intensive field campaigns. The system can also be used as a test-bed for the evaluation of lidar technologies for space-application.

This DIAL system leverages 2-micron laser technology developed under a number of NASA programs to develop new solid-state laser technology that provides high pulse energy, tunable, wavelength-stabilized, and double-pulsed lasers that are operable over pre-selected temperature insensitive strong CO₂ absorption lines suitable for profiling of lower tropospheric CO₂. It also incorporates new high quantum efficiency, high gain, and high signal-to-noise ratio phototransistors, and a new receiver/signal processor system to achieve high precision DIAL measurements. In situ sensor system calibration is in progress at Pennsylvania State University for field evaluation of the DIAL system in 2008. High-resolution laser spectroscopic measurements are being conducted at the Jet Propulsion Laboratory to characterize line parameters of the temperature insensitive line to be used for DIAL measurements.

Atmospheric tests of the laser have been conducted by operating it locked to the CO₂ absorption line center, with offset locking in the side-line mode, and in the off-line position. The reference laser is locked to center of absorption line within 390 kHz. This improves the level of stabilization ~~improved~~ by factor of 10 compared to earlier configuration. The detector has been characterized in the

laboratory and has been evaluated by conducting atmospheric tests at NCAR, Boulder, Colorado. The receiver uses an F2.2 all aluminum 16" diameter telescope and optical design focuses light onto a 200-micron detector. Design, development, atmospheric testing, and performance evaluation associated with the development of this DIAL system are presented in this paper.

I. INTRODUCTION

The atmospheric burden of CO₂ is increasing in response to widespread anthropogenic combustion of fossil fuels. Roughly half of the emitted CO₂ is absorbed by the Earth's oceans and terrestrial ecosystems [1]. This uptake [2] varies annually from 1 to 6 PgC yr⁻¹. Understanding source/sink processes and the geographic patterns of carbon fluxes are primary goals of carbon cycle science. Uncertainty in predictions of the carbon cycle is one of the leading sources of uncertainty in projections of future climate [3]. A double-pulsed DIAL system operating in the 2.05 micron band of CO₂ is being developed for profiling CO₂ in the low-to-mid troposphere. There are several advantages of this system over passive remote sensing systems including day/night operation, reduction or elimination of interference from clouds and aerosols, and direct and straight forward inversion that leads to better quality data and faster retrievals with few assumptions. A ground-based lidar profiling system with ability to delineate atmospheric boundary layer (ABL) CO₂ from the free tropospheric CO₂ is needed that can operate during day or night. CO₂ distributions in the troposphere are linked to transport and dynamical processes in the atmosphere and are associated with near-surface sources and sinks. Annually averaged, inter-hemispheric, and continental to marine boundary layer CO₂ mixing ratio differences are on the order of 1 to 3 ppm [4]. Thus 0.2 ppm has long been a benchmark for required instrumental precision. Achieving this level of precision is difficult with remote sensors. Much larger mixing ratio differences emerge,

however, at smaller spatial and temporal scales. In many instances exchange of ABL CO₂ with the free troposphere takes place through convective activity and passage of weather fronts. Hurwitz et al. [5], describe several synoptic passages and document 10 to 20 ppm mixing ratio changes that result from frontal passages. Thouret et al. [6], have shown that there is a high probability of observing more than one layered structure above the boundary layer at any time. Airborne sampling shows that the majority of the vertical structures in CO₂ mixing ratios are found within the lowest 5 km of the troposphere [4]. Thus, the requirements of this DIAL system development are: 0.5% (1.5 ppm) precision for vertical differences in the 30 minute mean mixing ratio resolved every 1 km from 0.5 to 5 km above ground.

Progress during the last year in the design, development, atmospheric testing, and performance modeling associated with the development of this DIAL system is presented in this paper. Field evaluation of the DIAL will be conducted in the third year of the project in coordination with field observations of the North American Carbon Plan (NACP) and OCO pre-validation activities.

II. THE CO₂ DIAL PROFILING SYSTEM

The DIAL system incorporates a high pulse energy, tunable, wavelength-stabilized, and double-pulsed laser that operates over a pre-selected temperature insensitive strong CO₂ absorption line in the 2.05- μ m band. It incorporates a newly developed low noise and high gain InGaAsSb/AlGaAsSb (AstroPower) infrared heterojunction phototransistor (HPT) with a 200 μ m sensitive area diameter. It is planned to operate it in the direct detection mode by taking advantage of a large 16" diameter telescope, which increases the photons collection at the detector by a factor of 16 over our previous system [7] in order to make CO₂ measurements above the boundary layer. The key lidar system parameters are given in Table 1. The Ho:Tm:LuLiF tunable laser is configured to operate at the 2053.204 nm CO₂ absorption line and later it is planned to operate it on the more temperature insensitive line [8] at 2050.967 nm using the Ho:Tm:YLF configuration. The CO₂ line will be fully characterized using a tunable high-resolution (New Focus Model #6335) laser diode at the Jet Propulsion Laboratory [9]. Accurate spectroscopic parameters will be derived that are critical to realizing ground-based CO₂ lidar detection strategy. The low-pressure line position is known to an uncertainty less than 6×10^{-5} cm⁻¹ [9]. The ambient temperature line strength will be determined to 2%, the line width to 3%, and the atmospheric pressure shift to 5×10^{-4} cm⁻¹ using a multispectral fitting technique.

TABLE I: LIDAR PARAMETERS

Parameters	Value	Unit
Pulse Energy	90	mJ
Pulse width	180	ns
Pulse repetition rate	5	Hz, doublets
Spectrum	Single frequency
On-line wavelength	2050.967	nm
Off-line wavelength	2051.017	nm
Beam quality	< 1.3 time diffraction limit
Long term (one hour) stability	< 2	MHz
Telescope Diameter	16	inch
Detector	AlGaAsSb/InGaAsSb Phototransistor

III. LASER DEVELOPMENT AND TESTING

Recent improvements in performance of the laser transmitter include double-pulse operation as demonstrated in the past with other DIAL systems. The double-pulse is injection seeded with the different on-off wavelength for each pulse of the doublet. The wavelength switching is accomplished by having two injection seed lasers that can be rapidly (in under 1 μ s) switched by an electro-optic device controlled by a simple logic signal. One of the seed lasers is tuned to the CO₂ line and the second is tuned to off line. The on-line laser is referenced to a CO₂ absorption cell at low pressure, and recent work has improved the performance of the wavelength locking to a level within 390 kHz standard deviation over hour-long time periods. This level of stabilization to line center reflects a factor of 10 improvements over our previous implementation, realized by converting to an external frequency modulation technique rather than wavelength dithering of the laser cavity length. An option now exists for tuning the on-line laser to the side of the line rather than the center of the line. By using the side of the absorption line, the optical depth of the DIAL measurement can be tailored for optimal performance. The side line reference is made by locking one seed laser onto line center and referencing a second laser to the center-line laser by monitoring the heterodyne beat signal between the two. A feedback loop, as shown in Fig. 1, has been implemented to lock the side-line laser to the center-line laser.

Electronic control holds an offset from center-line locked laser. Offset can be electronically programmed and laboratory tests have assessed quality of offset lock set upto for 2.8 GHz (37.3 pm). Atmospheric tests were conducted in a zenith-pointing mode at NASA Langley during the summer of 2006 using the heterodyne

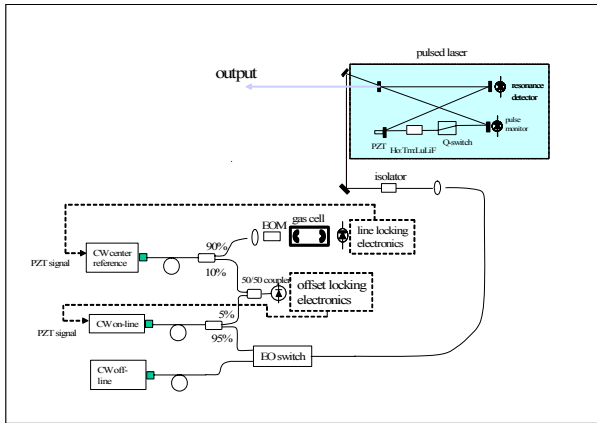


Fig. 1. Block diagram of injection seeded Ho:Tm:LuLiF laser; injection seeding setup with line center locked to the CO₂ line, side-line with offset locking with reference to the line and an off line away from the absorbing line is shown the lower portion of the figure.

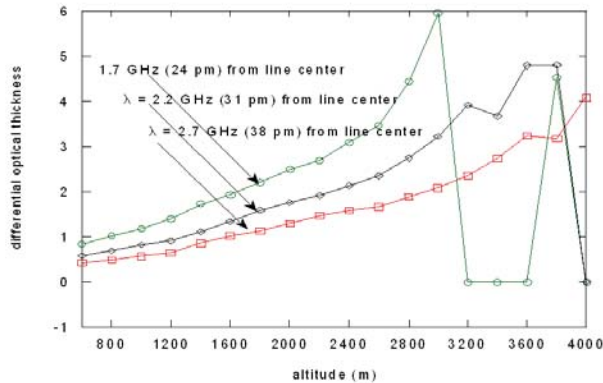


Fig. 2. Atmospheric tests to measure differential optical depths using changing side-line tuning.

detection system to test the ability to operate in the side-line mode. Fig. 2 shows the results of measurements of differential optical thickness as a function of altitude. The side-line was used as online and 3 different side-line positions were used that were offset by 24, 31, and 38 pm from line center. These results indicate ability to operate the laser in the sideline mode to optimize performance by tuning the sideline to desired absorption. Quantitative CO₂ measurements in the atmosphere were made on March 23, 2007 in the boundary layer using the Ho:Tm:LuLiF laser and the existing heterodyne detection system. These DIAL measurements are compared with in situ gas analyzer (LI-COR 6252, [10]) and are shown in Fig. 3. Offset between two caused by uncertainty in our knowledge of the spectroscopic constants. This problem is being addressed [10]. The two sensors show the same trend and occurrence of CO₂ perturbations and DIAL data show excellent precision. These measurements validate the operation of the laser system.

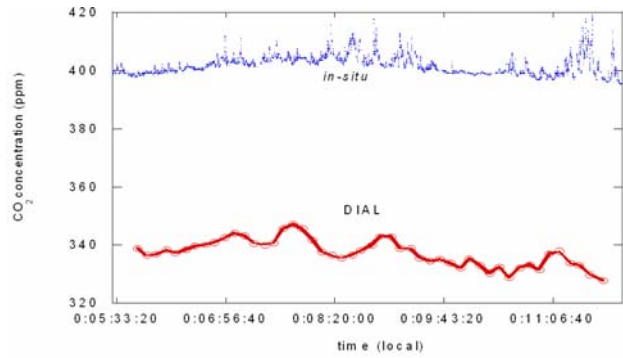


Fig. 3. Comparison of DIAL measurements using the Ho:Tm:LuLiF laser with measurements using an in situ gas analyzer.

IV. DETECTOR SYSTEM INTEGRATION AND ATMOSPHERIC TESTS

There are no detectors available commercially that can meet the requirements of the DIAL system under development. An ideal detector would be an avalanche photodiode (APD) that have high efficiency (QE~70%), high gain (~100) with low noise (NEP~ 2×10^{-14} W/Hz^{1/2}) and excess noise factor of < 2.0, high bandwidth (> 1 MHz), and fast settling time (1-3 micro seconds). A newly developed phototransistor (InGaAsSb/AlGaAsSb; AstroPower) with a 200 μ m sensitive area diameter and 400 μ m with mesa area diameter was used as the detector of choice [11]. The advantages of the phototransistor are its high gain (up to 3000), lower noise equivalent power (NEP), and higher quantum efficiency (~90%) compared to the traditional extended wavelength PIN photodiodes. These detectors are sensitive over the wavelength region 1.5 to 2.2 microns with peak performance near 2.05 micron. Characterization results of these detectors showed high gains (~3000) with lower bandwidth and longer recovery time. To capture rapid variations of signals in the lower troposphere, a low gain setting for the phototransistor will be required for the near field and a high gain setting for the far field. Post detector electronics circuit was developed that consists of analog and digital electronic circuit elements. Fig. 4 shows the configuration of the detection system electronics. The features of detection system electronics are:

- Computer controlled detector bias and temperature control electronics.
- Trans-impedance amplifier with dark current compensation.
- Voltage amplifier with offset and gain adjustments.
- State-of-the-art waveform 24-bit digitizer (National Instruments PXI-5922).

The capability of the detector system and its applicability to this program could not be demonstrated at Langley (receiver system is still under development). High sensitivity Aerosol Scanning Lidar (REAL:

Raman-shifted Eye-safe Aerosol Lidar)) system [12] of National Center for Atmospheric Research (NCAR) at Boulder, CO, was used for atmospheric testing by integrating newly developed phototransistors (HPT) into REAL system. The REAL system has a 16" telescope, two 200-micron APD detector channels, and operates at 1.543-micron wavelength. Atmospheric tests of the detector system were conducted at NCAR initially in June 2006 and later in December 2006 to test the HPT. The 200-micron HPT was used in one of the APD channels and the other APD was used as a reference in the other channel. While the HPT detector is not optimum at 1.543-micron, still, the first atmospheric tests in June 2006 indicated that the HPT has sensitivity to detect atmospheric features (cloud and aerosol layers) to altitudes > 5 km. This was the first time a HPT was used in a lidar system [13]. These tests showed that the HPT could resolve atmospheric features ~100 m in size (even for the 3 V high-gain setting at 20 °C). However, the HPT detection system showed overshoot that obscured measurements up to 3 km. Since the HPT itself had not shown an overshoot before, therefore, amplifier circuit following the HPT was a suspect.

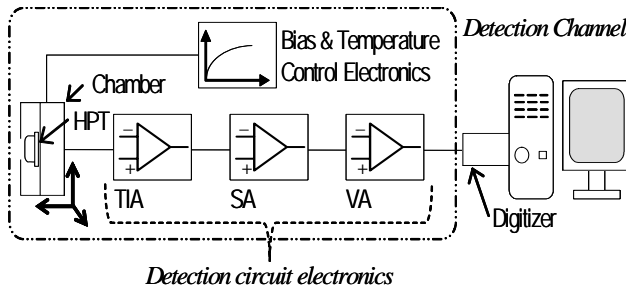


Fig. 4. Block diagram of detector system electronics.

Electronic trouble-shooting was performed on the TIA circuit at NASA LaRC. This investigation indicated that the detector's bias node required a large capacitance to stabilize the bias junction. An improved circuit with a stabilizing capacitor was used in the circuit. Results of overshoot (blue) and the improved performance (pink) using the new circuit are shown in Fig. 5. When a 1 mW optical pulse was applied to the phototransistor without the proper capacitance, a long undershoot occurs (70 μ sec), which in a lidar system will cause masking of measurements in the near field (up to about 3 km). Therefore, near field data for the first trip at NCAR was compromised. The problem was corrected for the second trip at NCAR. Fig. 6 shows comparison of measurements with the test detector (HPT) with the standard InGaAs APD at NCAR at 1.543-micron wavelength. Clearly in the near field overshoot problem is eliminated and boundary layer features are recovered compared to the measurements during the period of June 6, 2006. However, lower bandwidth and slower recovery problems cause systematic effects in data from the HPT

system compared to the APD system as illustrated in data from a far field thin cirrus cloud at 10-11 km range shown in Fig. 7.

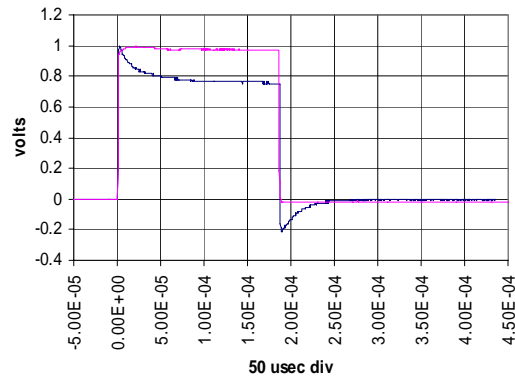


Fig. 5. Improved performance of circuit with the addition of a large capacitor (pink trace) compared with performance during tests at NCAR (blue trace).

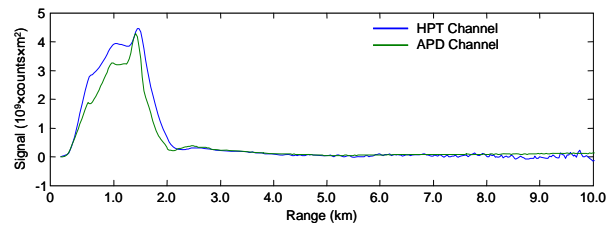


Fig. 6. Lidar measurements from the test (HPT) detector compared with results from APD detector system. The lidar was pointing with an elevation angle of 20 degrees.

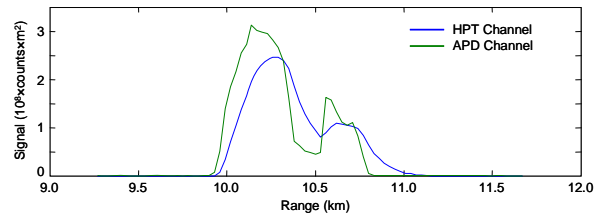


Fig. 7. Lidar measurements in the far field with the HPT and APD detector system compared. Lidar was pointing in the zenith direction.

To minimize systematic effects due to the bandwidth and slow recovery and to retrieve atmospheric lidar data from the HPT channel further lab characterization was conducted at NCAR including impulse response tests using short (0.1 μ s) pulse laser and dynamic linearity tests using simulated lidar signal profiles [14]. Data from the impulse response tests were used to deconvolve measurements from the HPT channel. An iterative convolution technique was employed that is a modification of a previously reported technique [15]. Results of deconvolution using this procedure are shown in Fig. 8 and 9 for both HPT and APD channels.

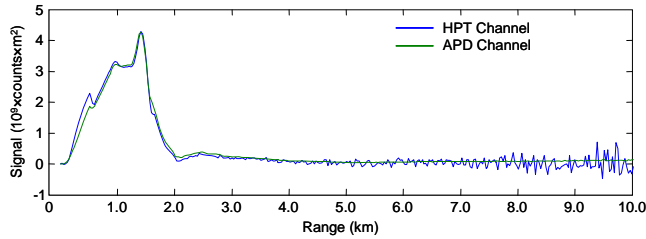


Fig. 8. Comparison of data from HPT and APD channels after deconvolution of the near field data.

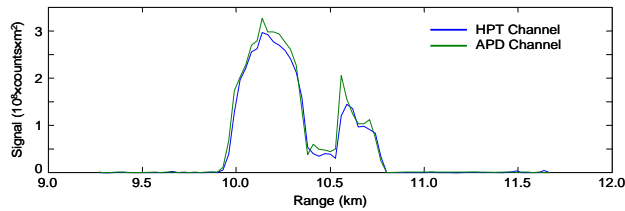


Fig. 9. Comparison of data from HPT and APD channels after deconvolution of the far field data. (Compare results with Fig. 7).

The deconvolution process eliminated recovery, increased resolution, and minimized phase delay between HPT and APD data channels as shown in Fig. 9 [14]. The deconvolution procedure was fast and was implemented for the whole series of measurements with consistent results [14]. Some degradation of signal-to-noise (S/N) in the low S/N regions was observed.

V. RECEIVER SYSTEM

Two receiver channels are planned to capture the full dynamic range of signals in the near (within the boundary layer 0.5 to 2.0 km range) and far field (above the boundary layer >1 km). The optical receiver uses a 16-inch diameter F/2.2 all aluminum telescope to minimize influences of thermal effects. The optical configuration of the receiver is shown in Fig. 10. The incident light is focused by the two mirrors of Cassegrain telescope through the pinhole and coupled into a fiber optic. The receiver optics includes a collimating lens, narrowband interference filter, focusing lenses, and protective window. A beam splitter is used to divide the radiation into two optical paths leading to detectors in the two channels. The optical design includes focusing the optical signal onto a spot diameter on the 200- micron diameter detector.

Finally, the collimating and focusing lenses are of a triplet (3 lenses) design and fabricated from SF11 optical glass. These will be custom coated use at 2-micron wavelength. Off-the-shelf interference filters and beam splitters are used in the design. A custom designed all aluminum telescope was manufactured by Welch Associates, Baltimore, MD. One of the specifications for this telescope was to have a small (45 micron diameter) focused area (blur spot size). Fig. 11 is a photograph of the 16" all metal telescope that was delivered to NASA Langley. This telescope, optics, detectors, and other

components would be placed inside an all-Aluminum box. This box would provide optical baffling and overall structural support.

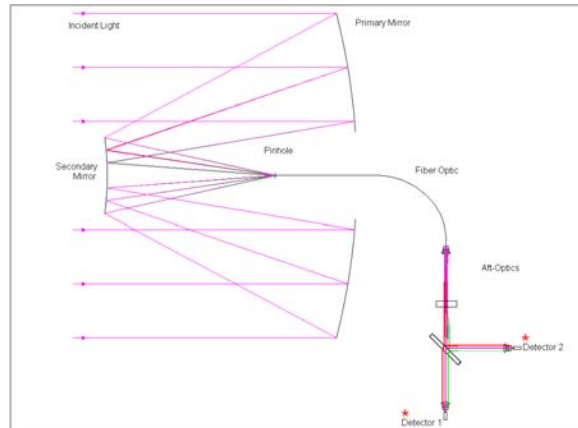


Fig. 10. Configuration of the optical design of the receiver system.

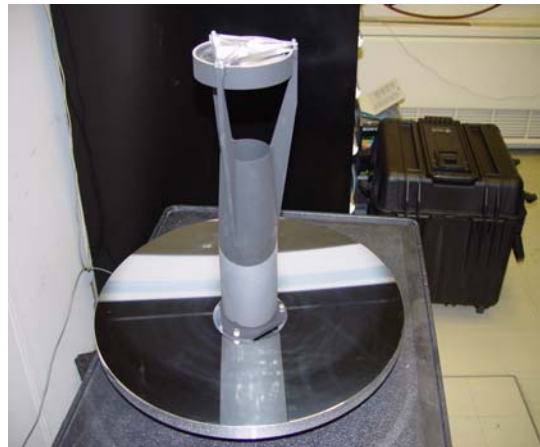


Fig. 11. Photograph of the 16" all aluminum telescope with a small blur spot diameter.

ACKNOWLEDGEMENT

This work is supported by 2- μm CO₂ DIAL IIP Project under NASA's Earth Science Technology Office. The authors would like to thank Terry Mack for developing phototransistor electronics and also optimizing post detector electronics; Bruce Barnes for development of data acquisition software; Stephanie Vay for providing in situ data for comparison with DIAL measurements; and Shane Mayor, Scott Spuler and NCAR management for their support and facilities for conducting detector tests at NCAR, Boulder, CO.

REFERENCES

- [1] Battle, M. et al., "Global carbon sinks and their variability inferred from atmospheric O₂ and δ¹³C", *Science*, **287**, 2467-2470, 2000.
- [2] Conway, T.J., et al., "Evidence for interannual variability of the carbon cycle from the National Oceanic and Atmospheric Administration/Climate Monitoring and Diagnostics Laboratory Global Air Sampling Network" *J. Geophys. Res.*, **99**, 22831-22855, 1994.
- [3] Friedlingstein, P. et al., "Positive feedback between future climate change and the carbon cycle", *Geophys. Res. Lett.*, **28**, 1543-1546, 2001.
- [4] Yi, C. et al., "The observed covariance between ecosystem carbon exchange and atmospheric boundary layer dynamics in North Wisconsin", *J. Geophys. Res.*, **109**(D08302): doi10.1029/2003JD004164, 2004.
- [5] Hurwitz, M.D. et al., "Advection of carbon dioxide in the presence of storm systems over a northern Wisconsin forest" *J. Atmos. Sci.*, **61**, 607-618, 2004.
- [6] Thouret, V. et al., "General characteristics of tropospheric trace constituent layers observed in the MOZAIC program", *J. Geophys. Res.*, **105**, 17,379-17,392, 2000.
- [7] Koch, G. J. et al., "Coherent differential absorption lidar measurements of CO₂", *Appl. Opt.* **43**, 5092-5099, 2004.
- [8] Menzies, R.T. and D.M. Tratt, "Differential laser absorption spectrometry for global profiling of tropospheric carbon dioxide: selection of optimum sounding frequencies for high-precision measurements", *Appl. Opt.*, **42**, 6569-6577, 2003.
- [9] Miller, C. E. et al., "Near infrared spectroscopy of CO₂ ¹⁶O¹²C¹⁶O line positions", *J. Mol Spectrosc.*, **228**, 329-354, 2004.
- [10] Vay, S.A. et al., "Airborne observations of the tropospheric CO₂ distributions and its controlling factors over the South Pacific basin", *J. Geophys. Res.*, **104**, 5663-5676, 1999.
- [11] Refaat, T.F. et al., "AlGaAsSb/InGaAsSb phototransistors for 2-μm remote sensing applications", *Optical Engineering*, Vol 43, No 7, 1647, 2004.
- [12] Mayor, S. and S. Spuler, "Raman-shifted eye-safe aerosol lidar", *Applied Optics*, **43**(19), 3915-3924, 2004.
- [13] T. Refaat, S. Ismail, T. Mack, N. Abedin, S. Mayor, S. Spuler, and U Singh, "Infrared Phototransistor Validation for Atmospheric Remote Sensing Application using the Raman-Shifted Eye-Safe Aerosol Lidar (REAL)", *Opt. Eng.* **46**(8), 2007 (in press).
- [14] Refaat, T., S. Ismail, N. Abedin, et al., "Lidar Backscatter Signal Recovery from Phototransistor Measurement Effects by De-convolution" (Manuscript in preparation), 2007.
- [15] van Cittert, P. "Zum einfluss der spaltbreite auf die intensitätsverteilung in spektallinien", *Z. Phys.* **69**, 298-308, 1931.